Available online at www.sciencedirect.com
ScienceDirect
Journal of Power Sources 163 (2007) 719–724
JOURNAL OF POWER SOURCES
www.elsevier.com/locate/jpowsour

Short communication

Effect of plasma nitriding on behavior of austenitic stainless steel 304L bipolar plate in proton exchange membrane fuel cell

R.J. Tian, J.C. Sun *, L. Wang

Institute of Materials and Technology, Dalian Maritime University, Dalian 116026, PR China

Received 9 October 2005; received in revised form 20 September 2006; accepted 22 September 2006
Available online 9 November 2006

Abstract

A dense and supersaturated nitrogen layer with higher conductivity is obtained on the surface of austenitic stainless steel 304L by the low temperature plasma nitriding. The effect of plasma nitriding on the corrosion behavior and interfacial contact resistance (ICR) for the austenitic stainless steel 304L was investigated in 0.05 M H_2SO_4 + 2 ppm F^- simulating proton exchange membrane fuel cell (PEMFC) environment using electrochemical and electric resistance measurements. The experiment results show that the stable passive film is formed after the potentiostatic polarization at the specified anodic or cathodic potentials under PEMFC operation condition, and the plasma nitriding improves slightly the corrosion resistance and decreases markedly the ICR of 304L. The ICR of the plasma nitrided 304L increases after the potentiostatic polarizations for 4 h, and lower than 100 mΩ cm^2 at the compaction force of 150 N cm^{-2}.

Keywords: Plasma nitriding; Austenitic stainless steel; Bipolar plate; Passive film; ICR

1. Introduction

Proton exchange membrane fuel cell (PEMFC) is an electrochemical device that converts directly and effectively the chemical energy stored in fuels into electrical energy. It is commercially viable power source for portable, stationary and transportation applications [1,2]. Single fuel cell unit can only provide very small power output voltage of about 0.6 V. To increase output power, individual fuel cells are connected into series using bipolar plates that are important multi-functional components for PEMFC stacks [3–5]. The functions of bipolar plates are: (1) connecting the individual fuel cells, (2) distributing fuel gas and oxygen (air) on the surfaces of the anode and cathode, (3) conducting the electrical current from the anode of one cell to the cathode of the adjacent, (4) supporting the membrane electrode assembly (MEA) and (5) providing rigidity for the PEMFC stacks.

Although the bipolar plate made from machined graphite has ideal performance for PEMFC, however, difficulty of fabrication process and high cost prevent it from large-scale development. In contrast to the traditional machined graphite [6,7], metals are attractive materials for bipolar plates as they have good conductivity and high strength and usually low gas permeability [8–10]. In addition, metals are easy to machine or stamp into thin sheets thus the overall cost and volume of the PEMFC stack are decreased [11–13]. Stainless steels, titanium, aluminum and other alloys may be used as the materials of bipolar plates. Among these metallic materials, austenitic stainless steels are strong candidates as a result of their relatively high strength, high chemical stability, ease of mass production and low cost. However, the electrochemical reactions in fuel cell, hydrogen protons in the anode and the moisture content in MEA make the solution acidic and aggressively corrosive. In H_2/air PEMFCs, the bipolar plates contact with the acidic solution containing F^-, SO_4^{2-}, SO_3^{2-}, HSO_4^-, CO_3^{2-} and HCO_3^-, etc. [14], whose pH value may change markedly under operation conditions. In the acidic PEMFC environment co-existing with water vapor and oxygen at high temperature, the austenitic stainless steels are certainly subjected to corrosion and form passive films on the surfaces. This passive film is electrically semiconductor and has higher electric resistance, resulting in the loss of output power of PEMFC stacks [8,12]. On the other hand, corrosion product (metal cations, especially in anode environment) could also poison the catalysts in membrane electrode assembly and lead

* Corresponding author. Tel.: +86 411 8472 7959; fax: +86 411 8472 7959.
E-mail address: sunjc@dlmu.edu.cn (J.C. Sun).

0378-7753/$ – see front matter © 2006 Elsevier B.V. All rights reserved.
doi:10.1016/j.jpowsour.2006.09.053

to the contamination of polymer electrolyte membrane and to lower the proton transfer rate, which will degrade certainly the power output of fuel cell during long-term operation [8,9,12]. In order to use the metals as bipolar plates in the PEMFCs and to enhance their performances, a conductive and protective coating has been used on the surfaces of bipolar plates by means of surface modification, such as physical vapor deposition (PVD) [11,15], chemical vapor deposition (CVD) [12], electroplating [13] and other methods [16,17], and the effect of coating on the performance has been evaluated in fuel cell unit tests. Up to now, the coatings of metallic bipolar plates have not proven sufficiently viable in the aggressive PEMFC environment since the inherent defects, such as micro-pores and micro-cracks, will cause local corrosion resulting in corrosion rate increasing with time.

To obtain the defect-free coatings, Brady et al. [18–20] proposed a gas thermal nitriding method to form a dense, continuous and protective CrN/Cr_2N nitride layer on the surface of Ni–50Cr bearing alloy. The results show that the corrosion resistance and surface conductivity of thermal nitrided Ni–50Cr alloy have been significantly improved even after the electrochemical polarization in 1 M H_2SO_4 + 2 ppm F^- solution. The discontinuous nitrided layer formed on the surface of 349^{TM} by thermal nitriding resulted in the poor corrosion resistance [16], while AISI446 treated by the same method has low ICR before and after polarization and low corrosion current density [17].

The corrosion resistance of Ni–Cr stainless steels is generally related to the contents of the nickel and chromium. The more the Cr contents in the stainless steel, the better its corrosion resistance. The higher contents of Ni and Cr cause the thinner oxide film, thus the better cell performance [8]. Sedriks [21] found that the corrosion resistance of the Ni–Cr austenitic stainless steels is improved as a result of the increase of N element by plasma nitriding. The conventional plasma nitriding method in the range from 500 to 600 °C can form a nitrided layer with the content of more than 20 at% N on the surface of austenite stainless steel, but deteriorates its corrosion resistance due to the formation of discontinuous and dispersive nitride precipitation in the nitrided layer and to the deficiency of Cr element in the substrate near the nitrided layer [22].

Faster diffusion rate and high quality adhesion are the dominant advantages of low temperature plasma nitriding, especially for the thin nitride layer. In order to understand the effect of plasma nitriding on performance of stainless steel 304L bipolar plates in the simulated PEMFC environments, polarization curves and potentiostatic polarization were measured by electrochemical method, and the ICR was evaluated after potentiostatic polarization under PEMFC operation condition in this work.

2. Experimental

2.1. Material and specimen preparation

The austenitic stainless steel 304L used in this work was melted in an induction vacuum furnace. The ingot with weight of 200 kg was homogenized at 970 °C, and was forged into bars with a diameter of 40 mm. The major chemical compositions (wt%) are: 0.016 C, 17.92 Cr, 10.14 Ni, 1.31 Mn and 0.47 Si. The bar was hot-forged into plates with a thickness of 5 mm, and then was solid-solution-treated at 1000 °C for 0.5 h and water-cooled. The specimens with a section of 1 cm^2 were prepared from this plate. The specimens were grounded with 280–1000# abrasive paper and polished mechanically. A part of them were used for low temperature plasma nitriding.

The glow discharge plasma nitriding was generated in an atmosphere of NH_3 by a pulse dc power supply. After nitriding at 370 °C for 2 h, the samples were cooled to the room temperature in vacuum condition. Structure of the plasma nitrided layer was examined by means of a type D/MAX-3B X-ray diffractometer and optical microscopy.

2.2. Electrochemical measurement

For electrochemical measurement, one side of the specimen for the studied 304L was connected to a copper wire for electrical connection, and then was covered with insulating epoxy. Only one side was left for exposure to the simulated solutions. Before the electrochemical measurements, the work side of each specimen was rinsed with alcohol.

Shores and Deluga [23] pointed out that the aqueous solution in operating H_2/air PEMFC stacks is acidic (pH 1–4) at beginning of operation and is almost near to pure water (pH 6–7) after some time of operation. The solution containing 0.05 M H_2SO_4 + 2 ppm F^- was selected to simulate the aggressive PEMFC environment in this work. The solution was prepared with analytical grade reagents and distilled water.

The electrochemical measurement was carried out in a type ZAHNER IM6e system controlled by a computer. A platinum sheet, saturated calomel electrode (SCE) and the specimen were used as the counter, reference and work electrode, respectively. The SCE was contacted with the solution by means of a Luggin capillary.

For the dynamic polarization experiment, the specimen was stabilized in the solution at open circuit until the change in potential was lower than 1 mV within 1 min. The scan potential was started from the potential lower than the open circuit potential to the anode polarized direction with the scanning rate of 1 mV s^{-1}. In order to investigate the stability of passive film formed on the surface of the plasma nitrided 304L, the potentiostatic polarization measurements were carried out at anode (around −0.1 V_{SCE}) and cathode (around +0.6 V_{SCE}) potentials. The solution was purged with H_2 or air at 70 °C during all electrochemical measurements.

2.3. Interfacial contact resistance (ICR)

The variation of ICR between passive film and carbon paper, $R_{C/PF}$, with compaction force was measured at room temperature according to the method described by Wang et al. [7]. The compaction force was applied by means of screwing a screw nut and lead screw, and the force was recorded with a MCK-C compaction sensor and a special force gauge. In order to reduce the heating effect of current, the electrical current of 100 mA was selected and provided by a type YJ-10A galvanostatic source.

The voltage across the thickness of specimen was measured by a Solartron 7081 type potentiometer with a precision of 10^{-8} V. The used measurement instruments and connective copper wires were unchanged during the measurement.

Since only one side of specimen was subjected to the electrochemical corrosion, the total measured resistance (R_{Total}) at the given compaction force is a sum of the resistance of measurement system (R_{System}), the bulk resistance of specimen (R_{Bulk}), the bulk resistance of Cu plates (R_{Cu}) and four interfacial components: two carbon paper/copper plate interface ($R_{C/Cu}$), carbon paper/passive film interface ($R_{C/PF}$) and carbon paper/air-formed oxidation film interface ($R_{C/SS}$). R_{Bulk} can be calculated from the resistivity of the untreated 304L measured by four-point probe method. The sum of R_{System} and R_{Cu} remained constant during the measurements. $R_{C/SS}$ for the untreated 304L and $R_{C/Cu}$ at the given compaction were measured under the same condition. Thus, $R_{C/PF}$ may be calculated from the measured R_{Total} at the given compaction.

3. Results and discussion

3.1. Microstructure of plasma nitrided layer

A low temperature plasma nitriding for austenitic stainless steels produces the nitrogen-enriched layers with higher nitrogen concentration over the temperature range of 350–420 °C. The thickness of the nitrided layer and nitrogen concentration depend primarily on the nitriding temperature, holding time and electric parameters.

The micrograph of plasma nitrided 304L at 370 °C for 2 h is shown in Fig. 1. A dense nitrided layer with thickness of 4–5 μm is formed on the surface. Fig. 2 gives the XRD pattern of plasma nitrided 304L. In addition to the diffraction peaks of austenite, there are two additional diffraction peaks. The indexing of these diffraction peaks indicates that a supersaturated nitrogen fcc phase, γ_N, is formed and its lattice parameter is larger than that of austenite. Furthermore, there are no diffraction peaks of nitrides CrN and Cr_2N, which show that only the dense nitrided layer of γ_N phase forms on the surface of substrate under the used condition of plasma nitriding.

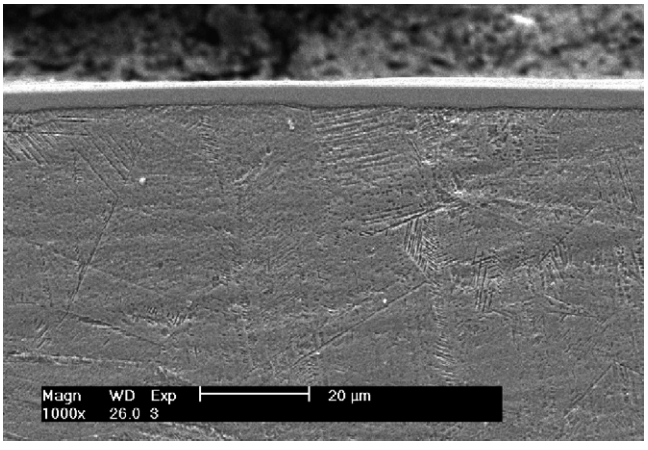

Fig. 1. Microstructure of the plasma nitrided 304L at 370 °C for 2 h.

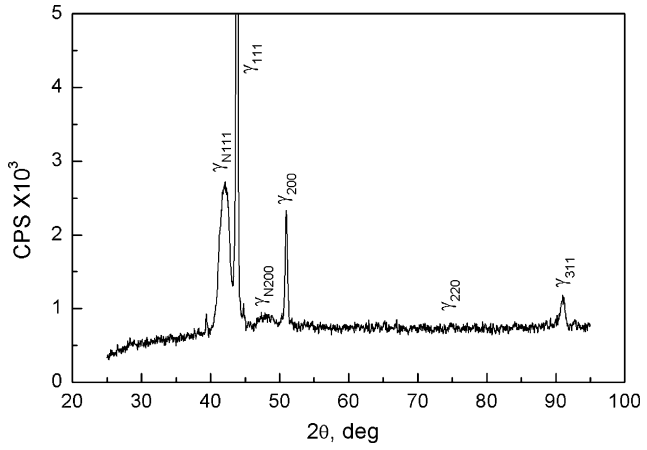

Fig. 2. XRD pattern of the nitrided layer for plasma nitrided 304L at 370 °C.

3.2. Polarization behavior

The polarization curves for the untreated and plasma nitrided 304L in 0.05 M H_2SO_4 + 2 ppm F^- at 70 °C are shown in Fig. 3. Both curves show similar passivation behavior. The free corro-

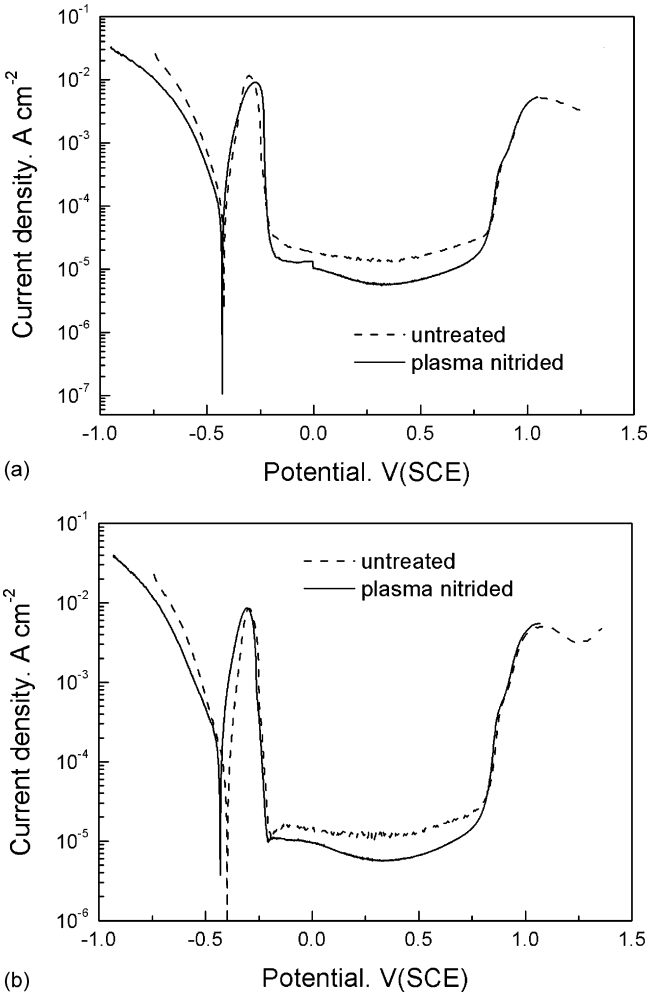

Fig. 3. Polarization curves for the untreated and plasma nitrided 304L in 0.05 M H_2SO_4 + 2 ppm F^- simulating PEMFC environments at 70 °C: (a) purged with H_2 and (b) purged with air.

sion potential, E_{corr}, for the studied 304L is close to −0.4 V_{SCE} in the simulated anodic or cathodic PEMFC environment. E_{corr} is not shifted markedly to positive direction by the low temperature plasma nitriding. When the potential is more than about +0.6 V_{SCE}, the current density increases rapidly as a result of the onset of transpassive region in which the passive film breaks down. The passive current density, independent of potential in the passivation ranges, for the plasma nitrided 304L is lower than that for the untreated one in the solution simulating PEMFC environments. The passive current density for the plasma nitrided 304L in the studied solution bubbled either with H_2 or air at 70 °C is lower than 16 μA cm^{-2}, which meet the goal of bipolar plates for PEMFC [24]. In addition, the anode (−0.1 V_{SCE}) and cathode (+0.6 V_{SCE}) operation potentials for PEMFC are also in passive regions, as shown in Fig. 3.

Since the passive film formed under application condition can affect the performance and lifetime of PEMFC, the potentiostatic polarization was conducted at −0.1 V_{SCE} in 0.05 M H_2SO_4 + 2 ppm F^- purged with H_2 at 70 °C for 4 h. The relationship between transient current density and time was recorded and shown in Fig. 4(a). It can be seen that transient current density first decreases markedly at the beginning of polarization, and then gradually stabilizes. This is affected by the formation of passive film. Once the stable passive film has covered the whole surface, the current will maintain a very low level.

The potentiostatic measurement was carried out at +0.6 V_{SCE} in the simulated solution purged with air. Fig. 4(b) shows the similar tendency to that shown in Fig. 4(a). However, the current density at −0.1 V_{SCE} purged with H_2 is higher than that at +0.6 V_{SCE} purged with air, which is in good agreement with the potentiodynamic studies. The time required to stabilize the passive film is different for the anodic and cathodic PEMFC environment, which may result from the difference in thickness and composition of the passive film. Similar results have been obtained in previous studies [16,17]. Compared to air-purged environment, the hydrogen-purged condition is more aggressive. The current densities were all lower than 16 μA cm^{-2} under both simulated PEMFC environments, and remain relatively stable and low level. The stable passive films were formed on the surface of the plasma nitrided 304L in the simulated PEMFC environments and prevented their further corrosion.

The above results show that the low temperature plasma nitriding is a promising method to improve the corrosion resistance of 304L in the simulated PEMFC environments.

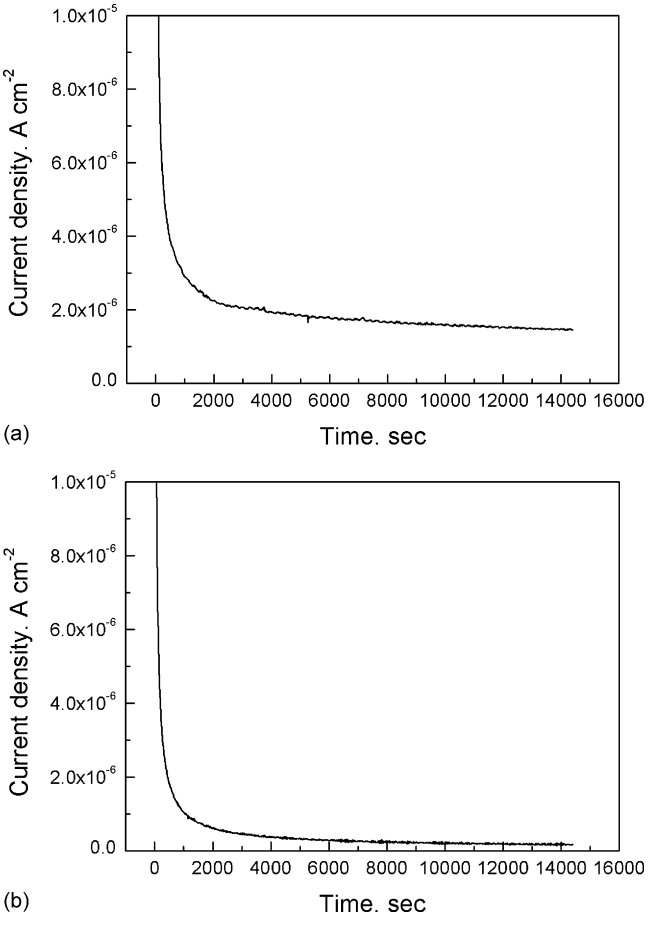

Fig. 4. Transient current of the plasma nitrided 304L in 0.05 M H_2SO_4 + 2 ppm F^- at 70 °C: (a) at −0.1 V_{SCE} purged with H_2 and (b) at +0.6 V_{SCE} purged with air.

3.3. Interfacial contact resistance

The ICR for bipolar plate often refers to the sum of all the resistances between the metallic sheet and the adjacent fuel cell component, typically a gas diffusion layer (carbon paper). The $R_{C/SS}$ for the plasma nitrided 304L as a function of compaction force is shown in Fig. 5. For comparison, the $R_{C/SS}$-compaction force curves for the untreated 304L and 316L, measured under the same condition, are also shown in this figure. It can be seen from Fig. 5 that the $R_{C/SS}$ decreases with increasing compaction force. With increasing compaction force between the specimen and carbon paper, the quantities of carbon–carbon and carbon–stainless steel contact points and the actual conductive area increase, which leads to a significant decrease in the $R_{C/SS}$. This result is similar to previous works [13,16,17,19,20]. At the same time, the ICR for the untreated 304L is lower than that for 316L over the range of applied compaction force as a result of its higher Cr content, which is consistent with the result

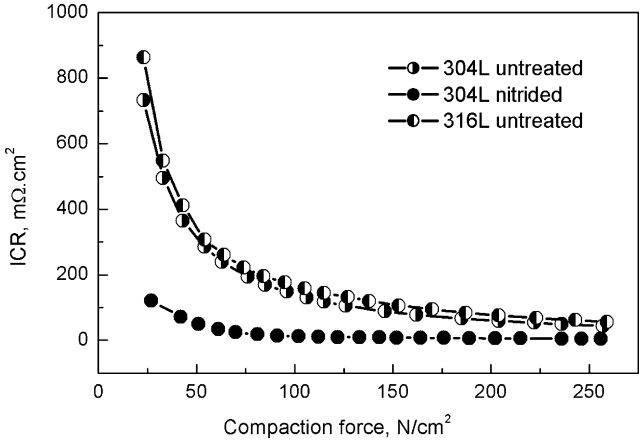

Fig. 5. Interfacial contact resistance of the untreated and plasma nitrided 304L as a function of compaction force.

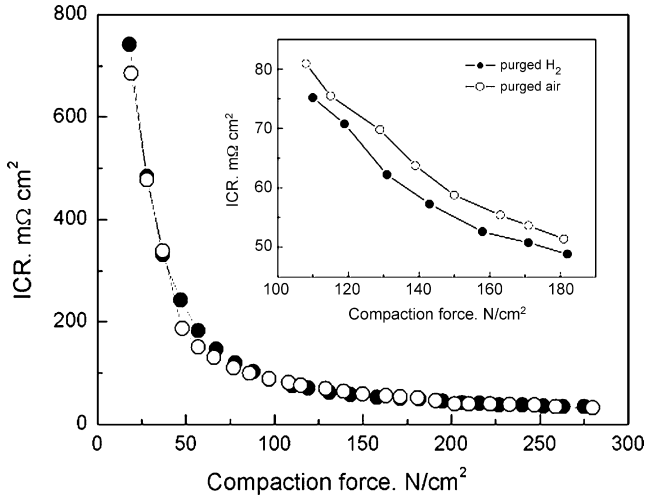

Fig. 6. Effect of potentiostatic polarization at operating potential on the interfacial contact resistance between carbon paper and passive film of the plasma nitrided 304L.

reported by Wang et al. [7]. The $R_{C/SS}$ of the untreated 304L is significantly decreased by the low temperature plasma nitriding, especially at the compaction force range (~100–150 N cm^{-2}) relevant to PEMFC stacks. The $R_{C/SS}$ for the plasma nitrided 304L is about 10 mΩ cm^2 at a compaction force of 150 N cm^{-2}, which is almost equal to that for the graphite. This result shows that the low temperature plasma nitriding has a beneficial effect on surface conductivity of 304L.

The passive film formed on the surface of stainless steel not only prevents further electrochemical corrosion, but also decreases the surface electrical conductivity. In other words, the passive film has a marked effect on the ICR, thus affecting the performance and lifetime of PEMFC. The passive film forms on the surface of the bipolar plates in PEMFC environments, and is different from that of the air-formed oxide film in the thickness and composition. Fig. 6 shows the variation of the $R_{C/PF}$ between the carbon paper and passive film with compaction force for the studied 304L. The $R_{C/PF}$ also decreases with increasing compaction force. Since the stable passive film formed during the potentiostatic polarization, the $R_{C/PF}$ for the plasma nitrided 304L increases also in comparison to that of the untreated 304L, however, the magnitude of increased $R_{C/PF}$ is very small. The air-formed film of stainless steel has a large amount of iron oxide, which acts as a dopant to chromium oxide. Films with high levels of iron oxides (higher doping) will have higher conductivity and lower resistance. In the passive film, with the depletion of iron from the film, the conductivity of the passive film is decreased and results in the increase of ICR. In other words, the composition of the passive film is mainly Cr_2O_3, and the iron oxides play only a minor role. Therefore, the conductivity of the air-formed film is superior to that of the passive film [25]. Flis and Kuczynska [26] found through XPS analysis that the passive film formed on the surface of the low temperature plasma nitrided 304L in 0.1 M Na_2SO_4 contained mainly Fe_3O_4/Fe_2O_3, with only a small amount of Cr_2O_3. In addition, the amount of iron oxides on nitrided steel was significantly larger than that on unnitrided steel. At same time, they pointed out that γ_N phase is resemble in approximation CrN and Cr_2N, respectively. On the other hand, the $R_{C/PF}$ for the plasma nitrided 304L were higher on the cathode side than on the anode side, and these differences were pronounced at lower compaction force. Wang and Turner [27] pointed out that the passive film formed in cathode environment is thicker than that formed in anode environment. For the plasma nitrided 304L applied the operation potential, $R_{C/PF}$ measured after potentiostatic polarization in the simulated PEMFC environments for 4 h are all lower than 60 mΩ cm^2, and higher than the goal of bipolar plates application.

The above results have shown that the plasma nitrided 304L can be an excellent candidate material as the bipolar plate for PEMFC stacks.

4. Conclusions

A dense γ_N phase layer with the higher conductivity is formed on the surface of the austenitic stainless steel 304L by the low temperature plasma nitriding. Electrochemical measurements are performed in 0.05 M H_2SO_4 + 2 ppm F^- at 70 °C bubbled either with H_2 or air to simulate PEMFC environment for bipolar plate application. The results show that the plasma nitrided 304L exhibits excellent corrosion resistance. The studies on the potentiostatic polarization show that the stable passive film is formed in the PEMFC environment at the operational potentials. The low temperature plasma nitriding improves significantly the surface conductivity. The ICR between the carbon paper and passive film for the plasma nitrided 304L increases slightly even after the polarizations at a specific operating potential for 4 h. This is related to the thickness, composition and structure of the passive film.

Acknowledgement

This work is supported by the National Natural Science Foundation of China (No. 10175012).

References

[1] J. Scholta, B. Rohland, V. Trapp, U. Focken, J. Power Sources 84 (1999) 231.
[2] E.A. Cho, U.-S. Jeon, H.Y. Ha, S.-A. Hong, I.-H. Oh, J. Power Sources 125 (2004) 178.
[3] H. Kuan, C. Chi, M. Ma, K. Chen, S. Chen, J. Power Sources 134 (2004) 7.
[4] M. Lee, L. Chen, Z. He, S. Yang, J. Fuel Cell Sci. Technol. 2 (2005) 14.
[5] D.P. Davies, P.L. Adcock, M. Turpin, S.J. Rowen, J. Appl. Elctrochem. 30 (2000) 101.
[6] J.S. Kim, W.H.A. Pelen, K. Hemmes, R.C. Makkus, Corros. Sci. 44 (2002) 635.
[7] H. Wang, M.A. Sweikart, J.A. Turner, J. Power Sources 115 (2003) 243.
[8] D.P. Davies, P.L. Adcock, M. Turpin, S.J. Rowen, J. Power Sources 86 (2000) 237.
[9] D.R. Hodgson, B. May, P.L. Adcock, D.P. Davies, J. Power Sources 96 (2001) 233.
[10] L. Ma, S. Warthsen, D.A. Shores, J. New Mater. Electrochem. Syst. 3 (2000) 221.
[11] S. Lee, C. Huang, J. Lai, Y. Chen, J. Mater. Process. Technol. 140 (2003) 688.

[12] J. Wind, R. Spah, W. Kaiser, G. Bohm, J. Power Sources 105 (2002) 256.
[13] S. Lee, C. Huang, J. Lai, Y. Chen, J. Power Sources 131 (2004) 162.
[14] Y. Li, W. Meng, S. Swathirajan, S. Harris, G. Doll, Corrosion Resistance PEM Fuel Cell US Patent 5,624,769 (20 April 1997).
[15] E.A. Cho, U.-S. Jeon, S.-A. Hong, I.-H. Oh, S.-G. Kang, J. Power Sources 142 (2005) 177.
[16] H. Wang, M.P. Brady, G. Teeter, J.A. Turner, J. Power Sources 138 (2004) 86.
[17] H. Wang, M.P. Brady, K.L. More, H.M. Meyer III, J.A. Turner, J. Power Sources 138 (2004) 79.
[18] M.P. Brady, K. Weisbrod, C. Zawodzinski, I. Paulauskas, R.A. Buchanan, L.R. Walker, Electrochem. Solid-State Lett. 5 (2002) A245.
[19] M.P. Brady, H. Wang, I. Paulauskas, B. Yang, P. Sachenko, P.F. Tortorelli, P.F. Tuner, R.A. Buchanan, Fuel Cell Sci. Eng. Technol. (2004) 437, 2503.
[20] M.P. Brady, K. Weisbrod, I. Paulauskas, R.A. Buchanan, K.L. More, H. Wang, M. Wilson, F. Garzon, L.R. Walker, Scripta Mater. 50 (2004) 1017.
[21] A.J. Sedriks, Corrosion 45 (1989) 510.
[22] L. Wang, Appl. Surf. Sci. 211 (2003) 308.
[23] D.A. Shores, G.A. Deluga, Handbook of Fuel Cell-Fundamentals, Technology and Applications, John Wiley & Sons, 2003, p. 273.
[24] V. Mehta, J.S. Cooper, J. Power Sources 114 (2003) 32.
[25] H. Wang, G. Teener, J. Turner, J. Electrochem. Soc. 152 (2005) B99.
[26] J. Flis, M. Kuczynska, J. Electrochem. Soc. 151 (2004) B573.
[27] H. Wang, J. Turner, J. Power Sources 128 (2004) 193.